

Supplemental Tables

Table S1. Top differentially methylated loci (in CpG islands of gene upstream regions) in CD14++CD16+ monocytes as compared to CD14++CD16- and CD14+CD16++ monocytes that are associated with miRNAs

Position	miRNA	CD14++CD16- NML	CD14++CD16+ NML	CD14+CD16++ NML	Prob CD14++CD16+ vs CD14++CD16- / CD14+CD16++	log2FC CD14++CD16+ vs CD14++CD16- / CD14+CD16++
chr16:33964507-33964512	miR-1826	1.2	240.1	2.4	1.000 / 1.000	7.6 / 6.7
chr20:26189837-26189842	miR-663	0.3	76.4	0.4	1.000 / 1.000	7.9 / 7.7
chr10:88126154-88126159	miR-346	0.3	4.7	0.3	0.998 / 0.997	4.1 / 3.9
chr8:124408332-124408337	miR-548d-1	0.1	4.0	0.2	0.997 / 0.994	4.8 / 4.2
chr1:154946769-154946774	miR-4258	0.2	4.2	0.4	0.997 / 0.994	4.1 / 3.5
chr4:144258110-144258115	miR-3139	0.1	3.7	0.1	0.995 / 0.993	5.1 / 5.1
chr4:174090079-174090084	miR-548t	0.4	4.2	0.5	0.996 / 0.992	3.6 / 3.2
chr6:31926803-31926808	miR-1236	0.3	3.7	0.2	0.994 / 0.993	3.7 / 4.6
chr15:70389830-70389835	miR-629	0.2	3.9	0.4	0.996 / 0.989	4.4 / 3.2
chr13:100259217-100259222	miR-4306	0.1	3.6	0.3	0.994 / 0.989	4.7 / 3.5
chr3:71633116-71633121	miR-1284	0.4	4.2	0.5	0.994 / 0.989	3.3 / 3.0
chr4:10118330-10118335	miR-3138	0.1	3.6	0.3	0.994 / 0.988	5.1 / 3.5
chr8:22102981-22102986	miR-320a	0.6	5.1	0.8	0.994 / 0.988	3.0 / 2.7
chr7:25990176-25990181	miR-148A	0.2	4.1	0.6	0.997 / 0.984	4.3 / 2.7
chr3:44803496-44803501	miR-564	0.5	3.8	0.3	0.989 / 0.992	3.0 / 3.8
chr8:22102516-22102521	miR-320a	0.1	3.4	0.3	0.992 / 0.986	4.6 / 3.7

chr19:797679-797684	miR-3187	0.1	3.2	0.2	0.991 / 0.987	4.9 / 4.4
chr11:79151421-79151426	miR-708	0.5	3.7	0.3	0.985 / 0.990	2.9 / 3.5
chr17:27224863-27224868	miR-144	0.2	3.2	0.3	0.989 / 0.984	3.7 / 3.6
chr2:208394814-208394819	miR-1302-4	0.3	3.3	0.3	0.987 / 0.985	3.4 / 3.6
chr3:15900694-15900699	miR-563	0.1	3.1	0.3	0.990 / 0.980	4.9 / 3.3
chr1:17186246-17186251	miR-3675	7.3	1.5	10.1	0.977 / 0.992	-2.3 / -2.7
chr15:42500209-42500214	miR-627	0.1	3.0	0.2	0.988 / 0.981	4.8 / 3.8
chr14:104584023-104584028	miR-3545	0.5	3.7	0.5	0.985 / 0.983	2.9 / 3.0
chr19:18392314-18392319	miR-3188	0.1	2.9	0.1	0.987 / 0.982	5.4 / 4.8
chr10:118927989-118927994	miR-3663	0.4	3.4	0.4	0.986 / 0.983	3.1 / 3.2
chr1:231175533-231175538	miR-1182	0.9	4.6	0.6	0.974 / 0.992	2.3 / 3.0
chr5:176057260-176057265	miR-4281	0.1	2.9	0.3	0.986 / 0.977	4.4 / 3.5
chr2:219263300-219263305	miR-26b	0.2	3.2	0.5	0.989 / 0.972	3.9 / 2.8
chr10:105991960-105991965	miR-609	0.5	3.3	0.4	0.978 / 0.982	2.7 / 3.2
chr17:74734005-74734010	miR-636	0.6	3.8	0.6	0.982 / 0.977	2.7 / 2.6
chr2:180726028-180726033	miR-1258	0.4	3.5	0.6	0.988 / 0.970	3.3 / 2.6
chr20:61807373-61807378	miR-124-3	0.7	4.2	0.7	0.981 / 0.976	2.6 / 2.5
chr10:98592490-98592495	miR-607	0.5	3.5	0.5	0.981 / 0.976	2.8 / 2.7
chr10:98592498-98592503	miR-607	4.5	0.8	4.5	0.980 / 0.975	-2.5 / -2.5

chr1:180471815-180471820	miR-3121	0.3	3.1	0.5	0.984 / 0.967	3.4 / 2.7
chr10:118927378-118927383	miR-3663	1.1	5.5	1.1	0.976 / 0.975	2.3 / 2.3
chr1:231175732-231175737	miR-1182	0.3	3.0	0.4	0.982 / 0.970	3.2 / 2.8
chr1:26856468-26856473	miR-1976	0.2	2.8	0.3	0.978 / 0.972	3.5 / 3.4
chr22:18257273-18257278	miR-3198	0.0	2.5	0.1	0.978 / 0.971	6.1 / 5.6
chr15:52587600-52587605	miR-1266	1.0	4.9	0.9	0.974 / 0.974	2.3 / 2.4
chr9:100174510-100174515	miR-1302-8	0.3	2.7	0.2	0.975 / 0.973	3.3 / 3.7
chr1:150521956-150521961	miR-4257	0.1	2.5	0.1	0.976 / 0.971	4.6 / 5.6
chr6:139013836-139013841	miR-3145	0.2	3.0	0.5	0.986 / 0.956	4.1 / 2.5
chr17:1082947-1082952	miR-3183	0.5	3.2	0.5	0.972 / 0.971	2.7 / 2.7
chr11:615841-615846	miR-210	0.1	2.4	0.1	0.974 / 0.966	5.1 / 4.5
chr10:6187086-6187091	miR-3155	0.2	3.0	0.5	0.986 / 0.953	4.1 / 2.5
chr7:25990927-25990932	miR-148a	0.1	2.5	0.3	0.976 / 0.963	4.2 / 3.3
chr14:31495944-31495949	miR-624	0.1	2.4	0.2	0.974 / 0.960	5.1 / 3.5
chr16:11439740-11439745	miR-548h-2	0.1	2.4	0.2	0.973 / 0.961	5.1 / 3.9

NML: normalized tag count (tags per million); Prob: probability; FC: fold change

Table S2. Differentially methylated loci associated with differential gene expression of corresponding genes¹

Position	Gene	Feature	Cpg island	CD14++CD16- NML	CD14++CD16+ NML	CD14+CD16++ NML	Prob CD14++CD16+ vs CD14++CD16- / CD14+CD16++	log2FC CD14++CD16+ vs CD14++CD16- / CD14+CD16++
chrX:47421025-47421030	ARAF	Intronic	Yes	0.1	1.4	0.3	0.906 / 0.851	4.3 / 2.4
chr2:219081875-219081880	ARPC2	Splicing	Yes	0.1	3.4	0.3	0.992 / 0.985	5.0 / 3.4
chr19:36630973-36630978	CAPNS1	UTR5	Yes	1.4	3.7	0.8	0.878 / 0.957	1.4 / 2.1
chr5:149792191-149792196	CD74	Exonic	No	0.5	2.6	0.9	0.944 / 0.840	2.4 / 1.4
chrX:47483357-47483362	CFP	downstream	Yes	0.0	1.0	0.0	0.858 / 0.842	4.8 / 5.2
chr20:23612769-23612774	CST3	downstream	No	0.0	1.0	0.0	0.860 / 0.842	5.8 / 5.2
chr20:23618673-23618678	CST3	Upstream	No	0.8	2.1	0.6	0.830 / 0.861	1.5 / 1.9
chr8:11725752-11725757	CTSB	Upstream	No	0.0	1.5	0.0	0.924 / 0.912	5.4 / 5.8
chr8:11725568-11725573	CTSB	UTR5	Yes	0.1	1.4	0.2	0.907 / 0.876	3.7 / 2.7
chr8:11725445-11725450	CTSB	Intronic	Yes	0.2	1.1	0.3	0.831 / 0.802	2.4 / 2.1
chr16:88717569-88717574	CYBA	Upstream	Yes	0.8	3.5	1.2	0.960 / 0.891	2.2 / 1.6
chr16:88717433-88717438	CYBA	UTR5	Yes	0.1	1.1	0.3	0.868 / 0.802	3.4 / 2.1
chr9:140009006-140009011	DPP7	Exonic	Yes	0.2	3.8	0.3	0.995 / 0.991	4.2 / 3.6
chr1:15737125-15737130	EFHD2	Intronic	Yes	0.8	4.5	0.4	0.977 / 0.996	2.5 / 3.6
chr17:39845739-39845744	EIF1	Intronic	Yes	0.2	2.7	0.3	0.977 / 0.970	3.5 / 3.4
chr11:67351087-67351092	GSTP1	UTR5	Yes	0.4	3.2	0.6	0.980 / 0.955	2.9 / 2.4

chr3:129033777-129033782	H1FX	UTR3	Yes	0.1	2.1	0.6	0.958 / 0.852	3.9 / 1.9
chr3:129033967-129033972	H1FX	UTR3	Yes	0.1	1.5	0.2	0.921 / 0.887	4.4 / 2.8
chr5:176325240-176325245	HK3	Intronic	No	0.0	1.2	0.1	0.891 / 0.866	5.1 / 3.5
chr1:23670944-23670949	HNRNPR	Upstream	Yes	0.1	3.1	0.5	0.988 / 0.969	4.5 / 2.7
chr1:23670821-23670826	HNRNPR	UTR5	Yes	0.2	2.9	0.4	0.983 / 0.965	3.8 / 2.8
chr11:117857361-117857366	IL10RA	Intronic	No	0.4	3.6	0.1	0.987 / 0.992	3.1 / 5.1
chr11:65381094-65381099	MAP3K11	Exonic	No	0.2	2.5	0.3	0.975 / 0.958	3.8 / 3.0
chr11:65381312-65381317	MAP3K11	UTR5	No	0.1	2.0	0.1	0.956 / 0.947	4.8 / 5.2
chr11:65381229-65381234	MAP3K11	UTR5	No	0.2	1.3	0.1	0.883 / 0.884	2.9 / 3.6
chr12:52419895-52419900	NR4A1	Intronic	No	0.1	2.9	0.3	0.986 / 0.977	4.8 / 3.5
chr12:52430738-52430743	NR4A1	Intronic	Yes	0.2	2.8	0.3	0.981 / 0.968	4.0 / 3.1
chr12:52445324-52445329	NR4A1	UTR5	Yes	0.6	3.7	0.7	0.975 / 0.962	2.5 / 2.3
chr12:52445909-52445914	NR4A1	Intronic	No	0.7	3.1	0.7	0.950 / 0.949	2.2 / 2.2
chr12:52431111-52431116	NR4A1	Intronic	Yes	0.7	2.9	1.2	0.942 / 0.840	2.1 / 1.3
chr22:44577638-44577643	PARVG	UTR5	No	0.2	2.9	0.3	0.983 / 0.976	3.8 / 3.5
chr22:44578783-44578788	PARVG	Intronic	No	0.1	0.8	0.1	0.825 / 0.812	3.6 / 4.0
chr4:84031265-84031270	PLAC8	Intronic	Yes	0.1	2.1	0.3	0.958 / 0.939	3.9 / 3.0
chr22:22307393-22307398	PPM1F	Upstream	Yes	0.4	1.9	0.4	0.906 / 0.890	2.3 / 2.2
chr12:131356337-131356342	RAN	Upstream	Yes	0.0	1.8	0.3	0.947 / 0.912	6.7 / 2.8

chr12:131356681-131356686	RAN	Intronic	Yes	0.1	0.9	0.0	0.842 / 0.834	3.7 / 5.1
chr2:20647209-20647214	RHOB	UTR5	Yes	0.2	3.6	0.2	0.993 / 0.991	3.9 / 4.1
chr2:20646754-20646759	RHOB	Upstream	Yes	0.2	2.6	0.2	0.976 / 0.968	3.9 / 3.6
chr2:20646885-20646890	RHOB	UTR5	Yes	0.1	2.6	0.4	0.979 / 0.957	4.6 / 2.8
chr2:20648257-20648262	RHOB	UTR3	No	0.9	3.1	0.8	0.903 / 0.902	1.8 / 1.9
chr2:20645445-20645450	RHOB	Upstream	No	0.1	1.3	0.1	0.892 / 0.884	3.2 / 3.6
chrX:128913986-128913991	SASH3	UTR5	No	0.0	0.9	0.1	0.840 / 0.822	4.6 / 4.1
chrX:23801135-23801140	SAT1	Upstream	Yes	0.3	1.7	0.2	0.915 / 0.923	2.6 / 3.5
chr17:80291263-80291268	SECTM1	Intronic	Yes	0.1	0.9	0.1	0.835 / 0.830	3.1 / 4.1
chr3:52530040-52530045	STAB1	Intronic	No	0.0	0.9	0.1	0.851 / 0.820	5.7 / 3.1
chr6:33281503-33281508	TAPBP	Exonic	Yes	0.3	3.2	0.3	0.985 / 0.981	3.3 / 3.3
chr16:30380792-30380797	TBC1D10B	Exonic	No	0.1	1.9	0.3	0.947 / 0.920	4.1 / 2.8
chr16:30381794-30381799	TBC1D10B	Upstream	Yes	1.6	6.4	2.5	0.957 / 0.900	2.0 / 1.4
chr16:30381533-30381538	TBC1D10B	Upstream	Yes	1.0	3.5	0.9	0.914 / 0.931	1.8 / 2.0
chr19:41858663-41858668	TGFB1	Exonic	Yes	0.0	2.9	0.1	0.987 / 0.982	7.3 / 5.8
chr19:41857378-41857383	TGFB1	Intronic	Yes	0.2	2.5	0.6	0.973 / 0.925	3.6 / 2.1
chr19:41859832-41859837	TGFB1	Upstream	Yes	0.1	1.7	0.2	0.939 / 0.923	4.0 / 3.5
chr19:41860253-41860258	TGFB1	Upstream	No	0.6	2.1	0.7	0.862 / 0.820	1.8 / 1.5
chr2:85132603-85132608	TMSB10	Upstream	Yes	0.0	0.9	0.1	0.851 / 0.830	5.7 / 4.1

chr6:28193242-28193247	ZNF193	Intronic	Yes	0.1	1.0	0.2	0.833 / 0.811	2.8 / 2.6
NML: normalized tag count (tags per million); Prob: probability; FC: fold change								

Table S3. Differentially methylated loci in uremic monocytes (in CpG islands of gene upstream regions) associated with cardiovascular disease (CVD), immune disease (IMM) and infection disease (INF)

Position	Gene	Control monocytes NML	Uremic monocytes NML	Prob	log2FC	CVD	INF	IMM
chr11:43702119-43702124	HSD17B12	0.1	7.8	1.000	-7.2	●	-	-
chr2:45878887-45878892	PRKCE	0.3	6.4	1.000	-4.6	●	-	●
chr10:94449085-94449090	HHEX	0.6	7.3	0.999	-3.6	●	-	●
chr22:50683474-50683479	TUBGCP6	0.1	4.2	0.998	-6.3	-	●	-
chr9:90112524-90112529	DAPK1	0.0	3.4	0.994	-7.0	●	-	-
chr5:10761675-10761680	DAP	0.7	5.1	0.992	-2.9	-	-	●
chr1:2344070-2344075	PEX10	0.1	1.9	0.965	-4.1	-	-	●
chr1:14026636-14026641	PRDM2	0.0	1.7	0.962	-6.0	●	-	-
chr7:45961262-45961267	IGFBP3	2.2	8.3	0.932	-1.9	●	●	●
chr19:531530-531535	CDC34	0.1	1.3	0.932	-3.6	-	-	●
chr2:133174115-133174120	GPR39	3.2	10.5	0.920	-1.7	●	-	-
chr1:32757466-32757471	HDAC1	1.5	0.3	0.907	2.2	-	-	●
chr21:28339999-28340004	ADAMTS5	0.2	1.2	0.900	-2.5	●	-	-

chr11:75917903-75917908	WNT11	1.3	0.2	0.897	2.4	●	-	-
chr18:7566650-7566655	PTPRM	0.0	0.9	0.888	-5.1	-	-	●
chr7:95025794-95025799	PON3	1.3	0.3	0.884	2.1	●	-	●
chr13:60738260-60738265	DIAPH3	1.5	0.4	0.878	2.0	●	-	-
chr6:168841817-168841822	SMOC2	1.0	0.1	0.878	2.7	●	-	●
chr15:27216006-27216011	GABRG3	1.9	4.2	0.862	-1.2	●	-	●
chr7:69062397-69062402	AUTS2	1.6	0.4	0.862	1.8	●	-	●
chr18:11981299-11981304	IMPA2	1.1	2.7	0.859	-1.3	●	-	-
chr11:61659297-61659302	FADS3	0.9	0.1	0.856	2.5	●	-	-
chr19:50879605-50879610	NR1H2	2.0	0.7	0.850	1.4	●	-	-
chr19:10527125-10527130	PDE4A	1.4	0.4	0.844	1.8	●	-	-
chr15:52311248-52311253	MAPK6	2.2	0.9	0.844	1.3	●	-	-
chr2:32390818-32390823	SLC30A6	1.0	0.2	0.844	2.0	-	●	-
chr8:55370263-55370268	SOX17	1.8	0.6	0.844	1.5	●	-	-
chr6:133562099-133562104	EYA4	0.8	0.1	0.842	2.4	●	-	-

chr2:21266951-21266956	APOB	1.5	0.5	0.836	1.6	●	●	●
chr6:33589066-33589071	ITPR3	0.6	0.0	0.834	3.7	-	-	●
chr3:53528641-53528646	CACNA1D	0.2	0.9	0.833	-2.1	●	-	●
chr12:48299276-48299281	VDR	1.7	0.6	0.833	1.4	●	●	●
chr11:123612389-123612394	ZNF202	1.4	0.4	0.832	1.6	●	-	-
chr18:25757801-25757806	CDH2	1.8	0.7	0.830	1.3	●	-	-
chr19:44439474-44439479	ZNF45	1.4	0.5	0.829	1.5	-	-	●
chr2:121102952-121102957	INHBB	1.9	0.8	0.829	1.2	●	-	-
chr6:71377392-71377397	SMAP1	1.6	0.6	0.828	1.4	-	-	●
chr10:1779970-1779975	ADARB2	1.7	0.6	0.826	1.4	●	-	-
chr21:42539687-42539692	BACE2	1.7	0.6	0.826	1.4	●	-	●
chr2:61292892-61292897	KIAA1841	1.7	0.6	0.826	1.4	-	-	●
chr7:51384812-51384817	COBL	0.5	1.5	0.825	-1.5	●	-	●
chr1:65432394-65432399	JAK1	1.5	0.5	0.825	1.5	-	●	●
chr19:29704312-29704317	UQCRFS1	1.8	0.7	0.824	1.2	-	●	-

chr10:94333920-94333925	IDE	0.9	2.1	0.823	-1.2	-	●	●
chr17:80709433-80709438	TBCD	0.7	1.7	0.823	-1.3	●	-	-
chr20:60795428-60795433	HRH3	0.1	0.6	0.822	-2.6	-	-	●
chr5:179719725-179719730	MAPK9	1.5	0.6	0.815	1.3	-	●	-
chr22:23487415-23487420	RAB36	1.5	0.6	0.815	1.3	●	-	-
chr1:201617348-201617353	NAV1	1.3	0.4	0.814	1.5	●	-	-
chr3:54155540-54155545	CACNA2D3	0.6	0.1	0.809	2.6	●	-	●
chr2:30454149-30454154	LBH	0.6	0.1	0.809	2.6	-	-	●
chr11:12132105-12132110	MICAL2	1.0	0.3	0.808	1.8	●	-	●
chr1:99127060-99127065	SNX7	1.4	0.6	0.808	1.3	-	-	●
chr3:183892601-183892606	AP2M1	1.7	0.7	0.808	1.2	-	●	-
chr11:65640514-65640519	EFEMP2	2.4	1.1	0.805	1.1	-	●	-
chr8:104511997-104512002	RIMS2	0.5	0.0	0.805	3.4	●	-	-
chr8:1772082-1772087	ARHGEF10	0.5	0.0	0.805	3.4	●	-	-
chr16:9058195-9058200	USP7	1.3	0.5	0.804	1.3	●	-	-

chr11:2465290-2465295	KCNQ1	0.8	1.8	0.803	-1.2	●	-	-
chrX:122866952-122866957	THOC2	0.6	0.1	0.803	2.1	-	●	-
chr5:109024967-109024972	MAN2A1	1.4	0.6	0.802	1.2	●	-	●
chr6:131456519-131456524	AKAP7	1.4	0.6	0.802	1.2	●	-	-
chr7:138666528-138666533	KIAA1549	1.5	0.6	0.802	1.2	●	-	-
chr1:77747641-77747646	AK5	0.7	1.6	0.800	-1.2	●	-	-

NML: normalized tag count (tags per million); Prob: probability; FC: fold change; CVD: cardiovascular disease; INF: infections; IMM: immune disease

Supplemental Figure Legends

Figure S1. Representative example of isolated monocyte subsets. Mean purity (\pm SD) of 7 isolations is given in each dot plot.

Figure S2. Interaction analysis of differentially methylated loci in intermediate monocytes. Interaction network was generated with the string database using most differentially methylated loci within CpG islands of gene upstream regions ($\text{Prob} \geq 0.95$) in intermediate monocytes as compared to classical and nonclassical monocytes. Shown are interactions at a confidence score of 0.9. In line with the proinflammatory and distinct role of intermediate monocytes in immunity, the interaction analysis of differentially methylated loci reveals a strong cluster containing genes linked to NF- κ B signaling (*RELA*, *NFKB1*, *NFKB2*), which are presented in the central position of the pathway analysis. In addition, several genes that are linked to transcriptional regulation (*STAT1*, *CEBPB*, *FOS*) are also located in this cluster. Gene ontology (GO) analysis of genes that are presented in this network confirm an enrichment of genes connected to regulation of gene expression, indicating that several remodeling processes are induced in intermediate monocytes. In line, further significant GO terms comprise cell differentiation and cellular biosynthesis processes.

Figure S3. Interaction analysis of selected pathways enriched in intermediate monocytes. Enrichment analysis was performed among genes with differentially ($\text{Prob} \geq 0.8$) methylated promoters in intermediate as compared to classical and nonclassical monocytes by using the WEBGESTALT platform. Genes enriched in the pathways “Immune System”, “TNF receptor

signaling pathway”, “Metabolism of lipids and lipoproteins” and “Cell cycle” were used as input to GeneMANIA to construct networks of interactions. Enriched functions in the networks were highlighted with the GeneMANIA module (“Immune System”: Antigen-receptor-mediated signaling pathway [yellow], Toll-like receptor signaling pathway [blue], Regulation of innate immune response [red]; “TNF receptor signaling pathway”: Immune response-regulating cell surface receptor signaling pathway [red]; “Metabolism of lipids and lipoproteins”: Triglyceride metabolic process [red]; “Cell cycle”: Cell cycle G2/M phase transition [blue], Cell cycle checkpoint [red]). In line with the interaction analysis that was generated with the string database (Figure S2), the cluster that contains genes linked NF-κB signaling (RELA, NFKB1, NFKB2) is also located at central positions within the networks “Immune System” and “TNF receptor signaling pathway”. The inflammatory potential of intermediate monocytes^{1,2} is supported by the enrichment of genes connected to the Toll-like receptor signaling pathway; the potential of intermediate monocytes for antigen processing and presentation^{1,3} is supported by the enrichment of genes connected to Antigen-receptor-mediated signaling pathway within “Immune System”. The pathway “Metabolism of lipids and lipoproteins”, which is enriched in intermediate monocytes, is in line with the distinct function of intermediate monocytes in the cholesterol metabolism.⁴ The three monocyte subsets represent different stages of monocyte differentiation⁵. The conversion of one subset to another requires regulation of cell differentiation and cell cycle, which involves genes that are differentially methylated in intermediate monocytes in comparison to classical and nonclassical monocytes.

Figure S4. Analysis of *in vitro* differentiated classical monocytes. Percentages of classical monocytes (left panel) as well as the capacity of classical monocytes to produce reactive oxygen species (middle panel) and to phagocyte (right panel) were determined with flow-

cytometry. Data are presented as means \pm SEM and compared by Student t test. *P<0.05. ROS indicates reactive oxygen species.

Figure S5. Methyl-Seq analysis of uremic monocytes. Schematic representation of differences in DNA methylation between monocytes which were differentiated under control or under uremic conditions. Presented are total loci (left panel) as well as loci within CpG islands of gene upstream regions (right panel). Loci with differential methylation are given as circles (Prob \geq 0.9 in red, Prob between 0.8 and 0.9 in black) and all other loci are given as grey dots.

Figure S6. Interaction analysis of differentially methylated loci in uremic monocytes.

Interaction network was generated with the string database using differentially methylated loci within CpG islands of gene upstream regions (Prob \geq 0.8) between control and uremic monocytes. Shown are interactions at a confidence score of 0.4. The interaction analysis of these differentially methylated loci reveals a strong cluster containing genes linked to regulation of gene transcription (*HDAC1*, *UBTF*, *SAP130*) and a second cluster containing genes linked to cell differentiation and cell proliferation (*FLT3*, *NOP2*, *RUNX1T1*), indicating that hematopoietic differentiation is disturbed under uremic conditions, which is in line with functional analyses (Figure 2B). A small cluster at the top of the interaction analysis contains genes linked to intercellular transport processes (*AP2M1*, *AP3M2*, *CLTB*), pointing towards different remodeling processes in control and uremic monocytes.

Figure S7. Hierarchical cluster analysis. Analysis was performed among those 10,000 loci with the highest tag count in the combined analysis that comprises both circulating classical, intermediate and nonclassical monocytes as well as *in vitro* generated monocytes.

Figure S78. Impact of C1 metabolites on monocyte subsets. Distribution of classical (left panel), intermediate (middle panel) and nonclassical monocytes (right panel) after stimulation of whole blood for 5h (upper panel) and 16h (lower panel) with increasing concentrations of homocysteine (30μM, 100μM and 500μM) or Adenosine-2',3'-dialdehyde (10μM and 50μM). Data are presented as mean±SEM of six (for 5h) and seven (16h) independent experiments. Statistical analysis was performed with one-way ANOVA followed by Dunnett's multiple comparison post hoc test. *P<0.05, **P<0.001.

Figure S89. Impact of C1 metabolites on CD16 and CD86 expression on total monocytes. Expression of CD16 (left panel) and CD86 (right panel) on total monocytes after stimulation of whole blood for 5h with increasing concentrations of homocysteine (30μM, 100μM and 500μM) or Adenosine-2',3'-dialdehyde (10μM and 50μM). Data are standardized to the control approach and presented as mean±SEM of six independent experiments. Statistical analysis was performed with one-way ANOVA followed by Dunnett's multiple comparison post hoc test. *P<0.05, **P<0.001.

Figure S910. Impact of C1 metabolites on CX3CR1 and CCR5 expression on total monocytes and monocyte subsets. Expression of CX3CR1 (left panel) and CCR5 (right panel) on total monocytes (upper panel) and monocyte subsets (lower panel) after stimulation

of whole blood for 5h with homocysteine (100 μ M) or Adenosine-2',3'-dialdehyde (50 μ M). Data are standardized to the control approach and presented as mean \pm SEM of six independent experiments. Statistical analysis was performed with one-way ANOVA followed by Dunnett's multiple comparison post hoc test. *P<0.05, **P<0.001.

Figure S101. Validation of the gating strategy. An additional gate was drawn within the gate which defines intermediate monocyte gate at close vicinity to the classical monocyte gate (red arrow) in the control (left panel) and stimulation approaches (right panel); within this gate, CCR5 expression was flow-cytometrically determined. Data are standardized to the control approach and presented as mean \pm SEM of six independent experiments. Statistical analysis was performed with one-way ANOVA followed by Dunnett's multiple comparison post hoc test.

Figure S112. Impact of C1 metabolites on monocyte subsets. ~~Correlation between nonclassical monocytes and homocysteine (left panel) as well as between nonclassical monocytes and S-adenosylhomocysteine (right panel) within the I Like HOME study. To allow better visualization, data from two participants (participant 1: plasma homocysteine 46.7 mmol/l; participant 2: plasma SAH 43.0 nmol/l) are not depicted in the figure, but included in all calculations. Correlation coefficients were calculated by Pearson test.~~ Association of nonclassical monocytes with homocysteine (left panel) and S-adenosylhomocysteine (right panel) within the I Like HOME study. Study participants were stratified into quartiles and data were analyzed with one-way ANOVA.

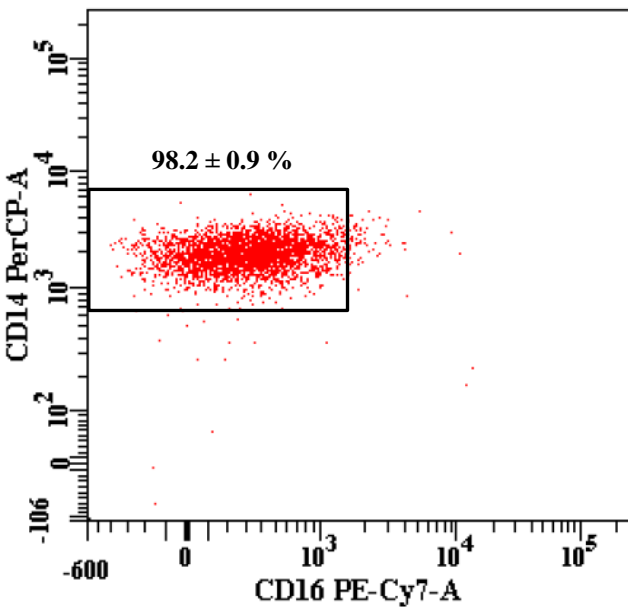
Figure S123. Impact of C1 metabolites on monocyte subsets. ~~Association of intermediate monocytes with homocysteine (left panel) and S-Adenosylhomocysteine (right panel) within the I Like HOME study. Study participants were stratified into quartiles and data were analyzed with one-way ANOVA.~~Correlation between intermediate monocytes and homocysteine (left panel) as well as between intermediate monocytes and S-adenosylhomocysteine (right panel) within the I Like HOME study. To allow better visualization, data from two participants (participant 1: plasma homocysteine 46.7 mmol/l; participant 2: plasma SAH 43.0 nmol/l) are not depicted in the figure, but included in all calculations. Correlation coefficients were calculated by Pearson test.

Supplemental References

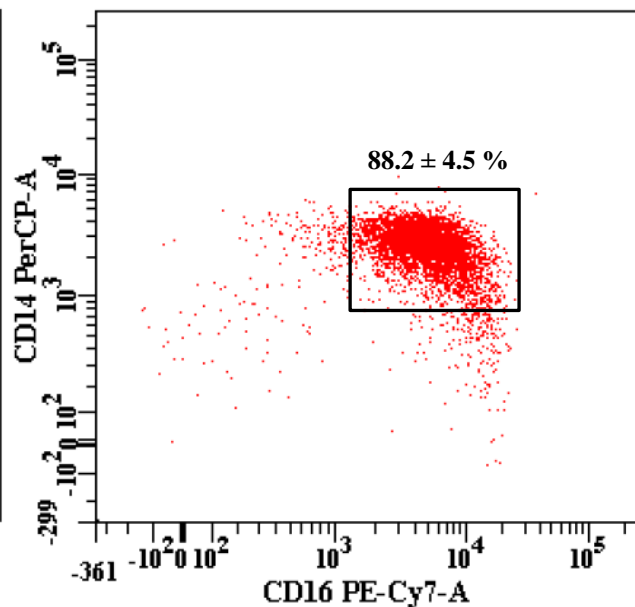
1. Zawada AM, Rogacev KS, Rotter B, et al. SuperSAGE evidence for CD14⁺⁺CD16⁺ monocytes as a third monocyte subset. *Blood*. 2011;118(12):e50-61.
2. Cros J, Cagnard N, Woollard K, et al. Human CD14^{dim} monocytes patrol and sense nucleic acids and viruses via TLR7 and TLR8 receptors. *Immunity*. 2010;33(3):375-386.
3. Wong KL, Tai JJ, Wong WC, et al. Gene expression profiling reveals the defining features of the classical, intermediate, and nonclassical human monocyte subsets. *Blood*. 2011;118(5):e16-31.
4. Rogacev KS, Zawada AM, Emrich I, et al. Lower Apo A-I and lower HDL-C levels are associated with higher intermediate CD14⁺⁺CD16⁺ monocyte counts that predict cardiovascular events in chronic kidney disease. *Arterioscler Thromb Vasc Biol*. 2014;34(9):2120-2127.
5. Rogacev KS, Zawada AM, Hundsdorfer J, et al. Immunosuppression and monocyte subsets. *Nephrol Dial Transplant*. 2015;30(1):143-153.

Supplemental Figures

Classical monocytes



Intermediate monocytes



Nonclassical monocytes

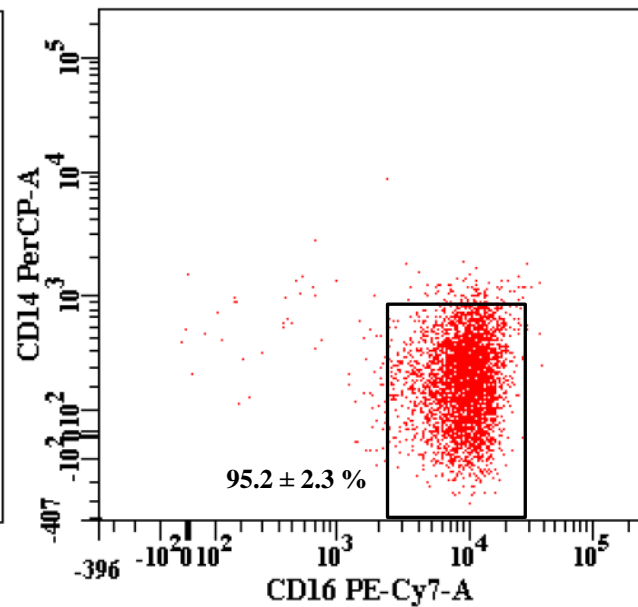
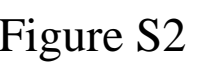
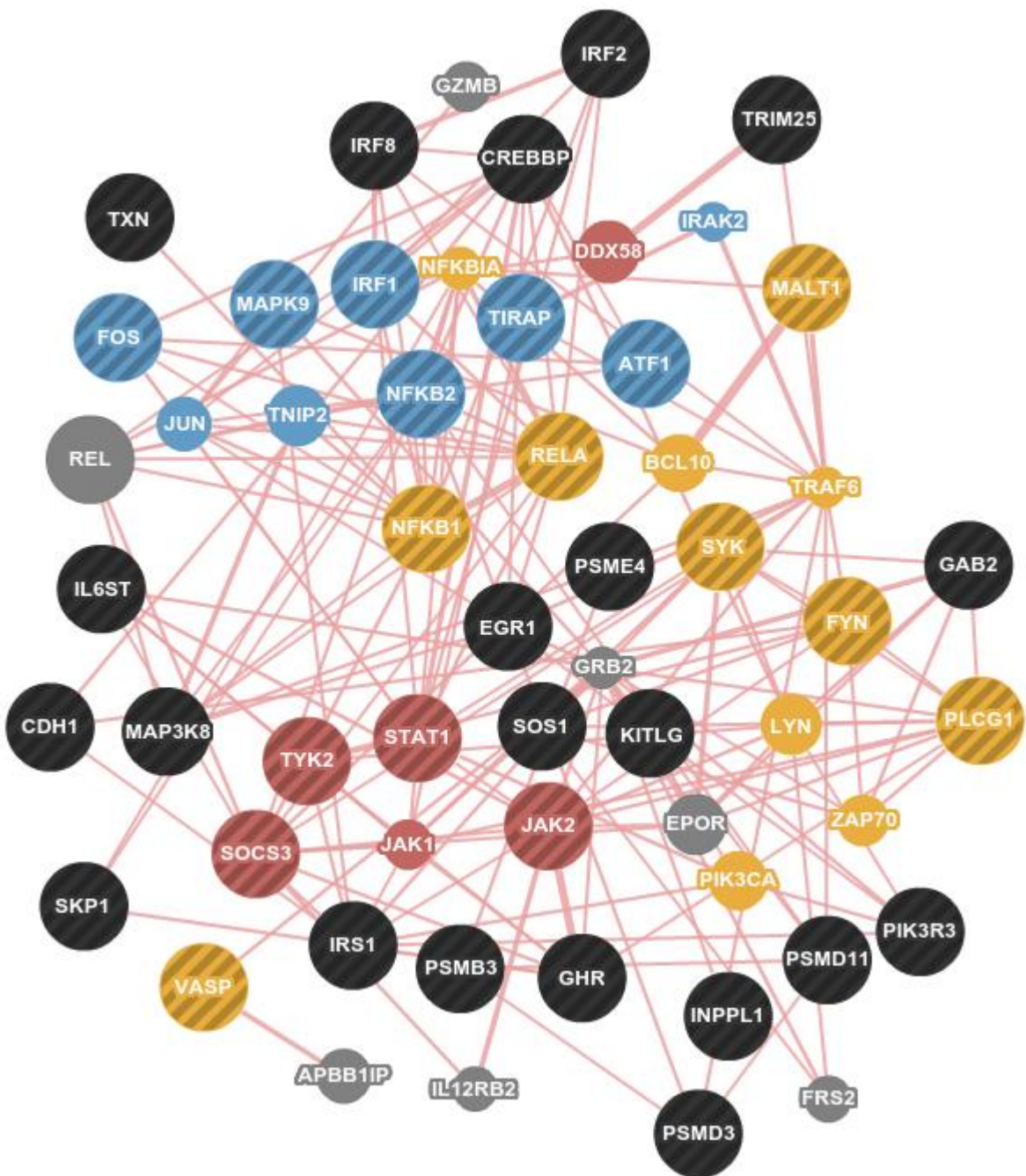


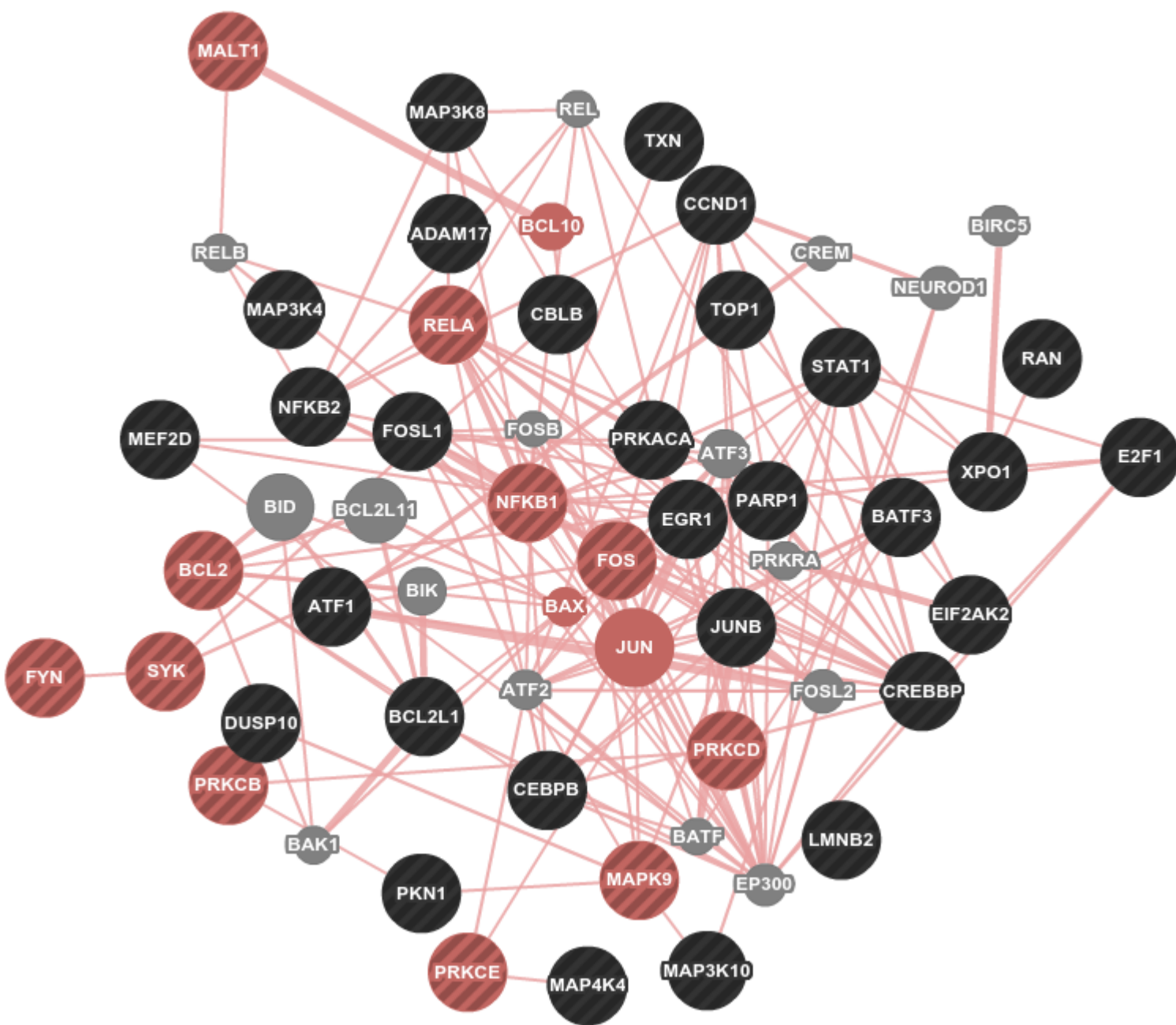
Figure S1



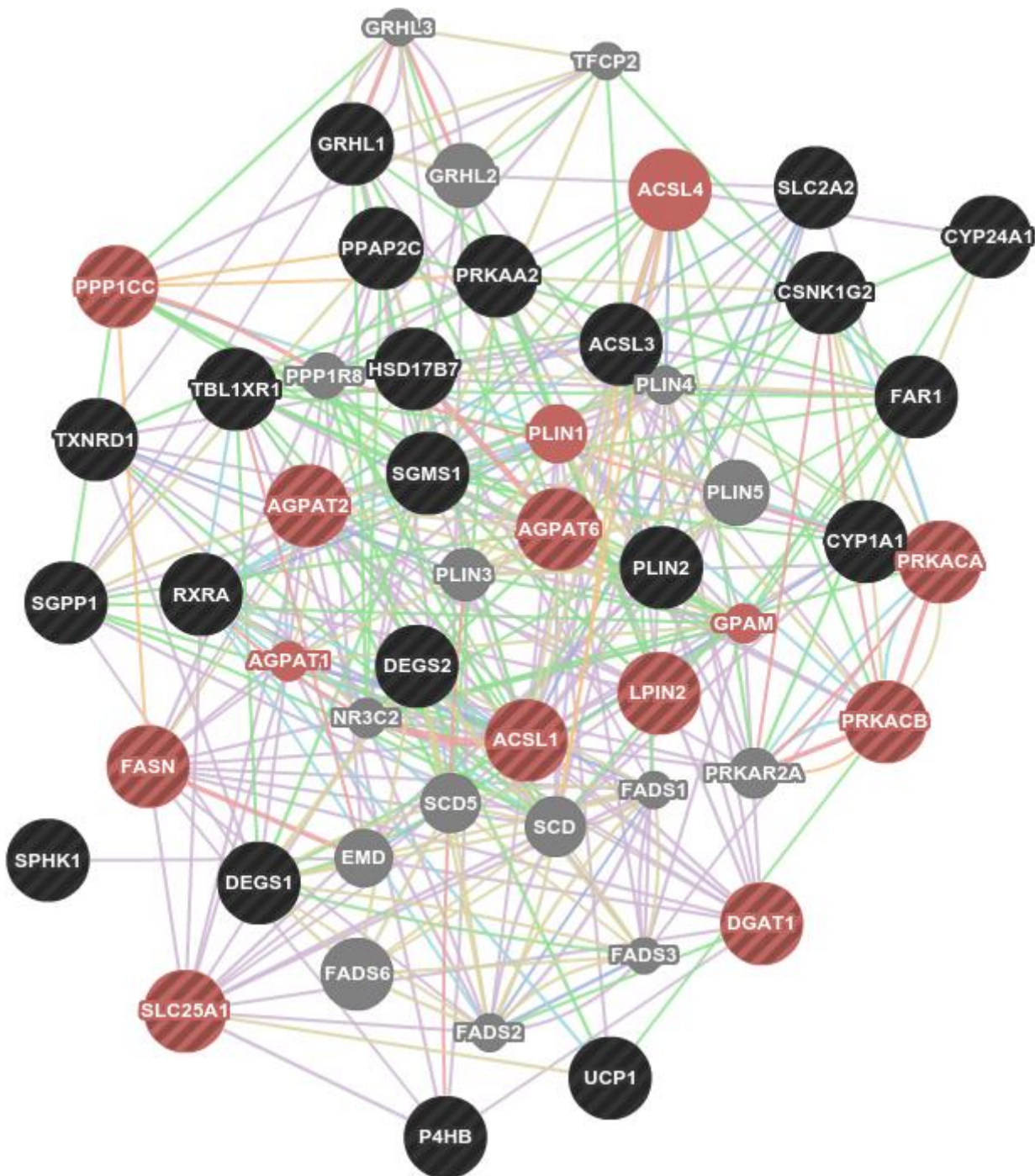
Immune System



TNF receptor signaling pathway



Metabolism of lipids and lipoproteins



Cell cycle

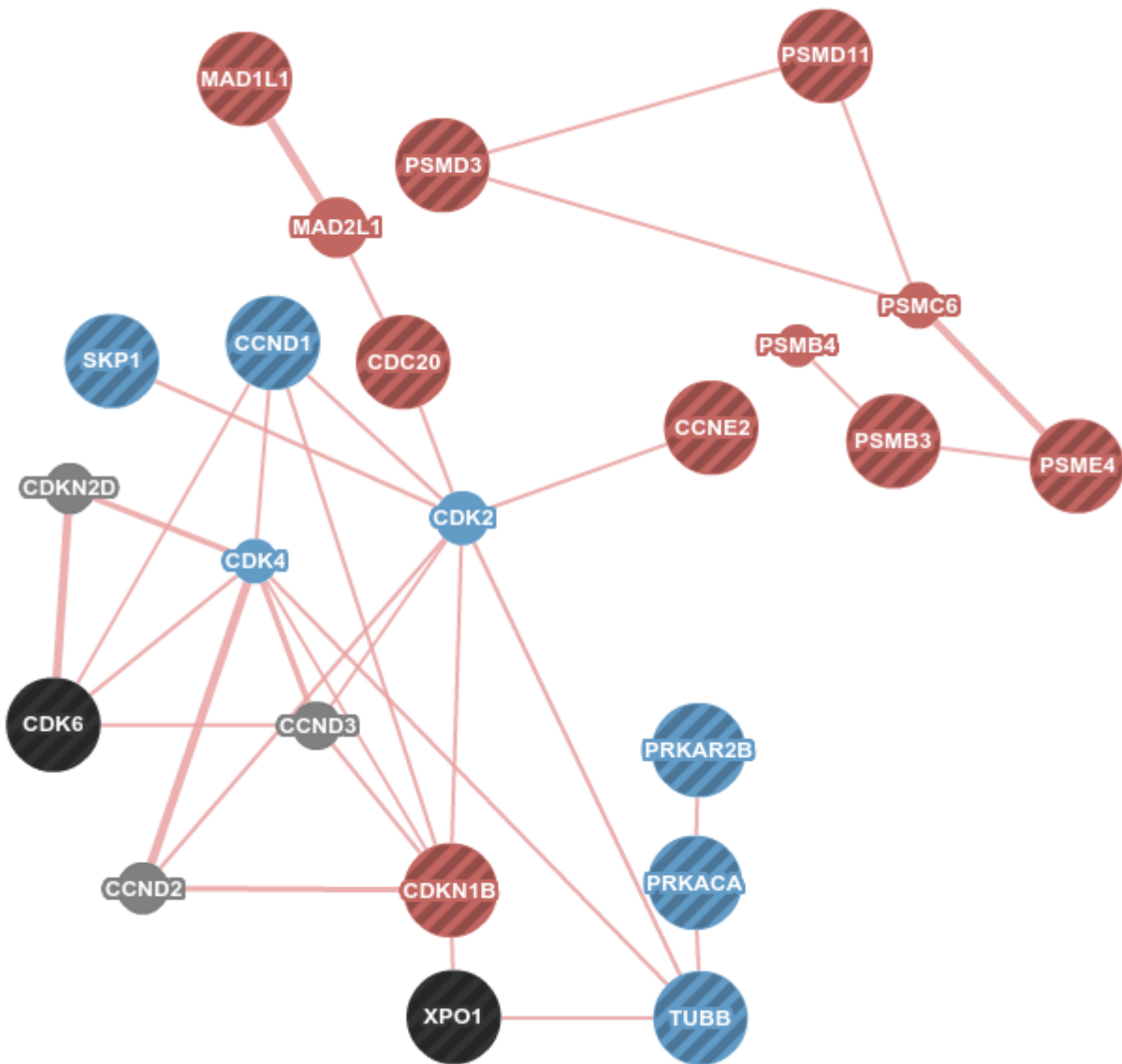


Figure S3

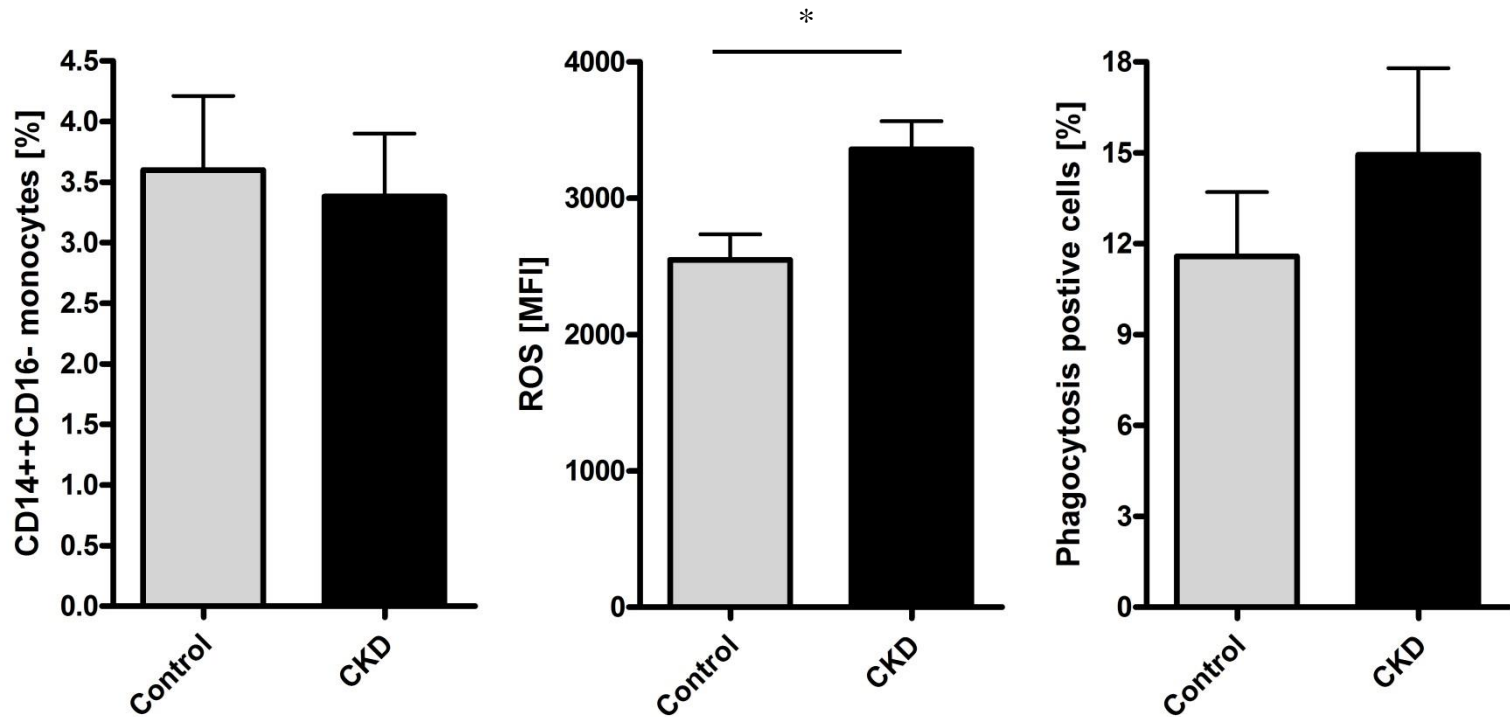
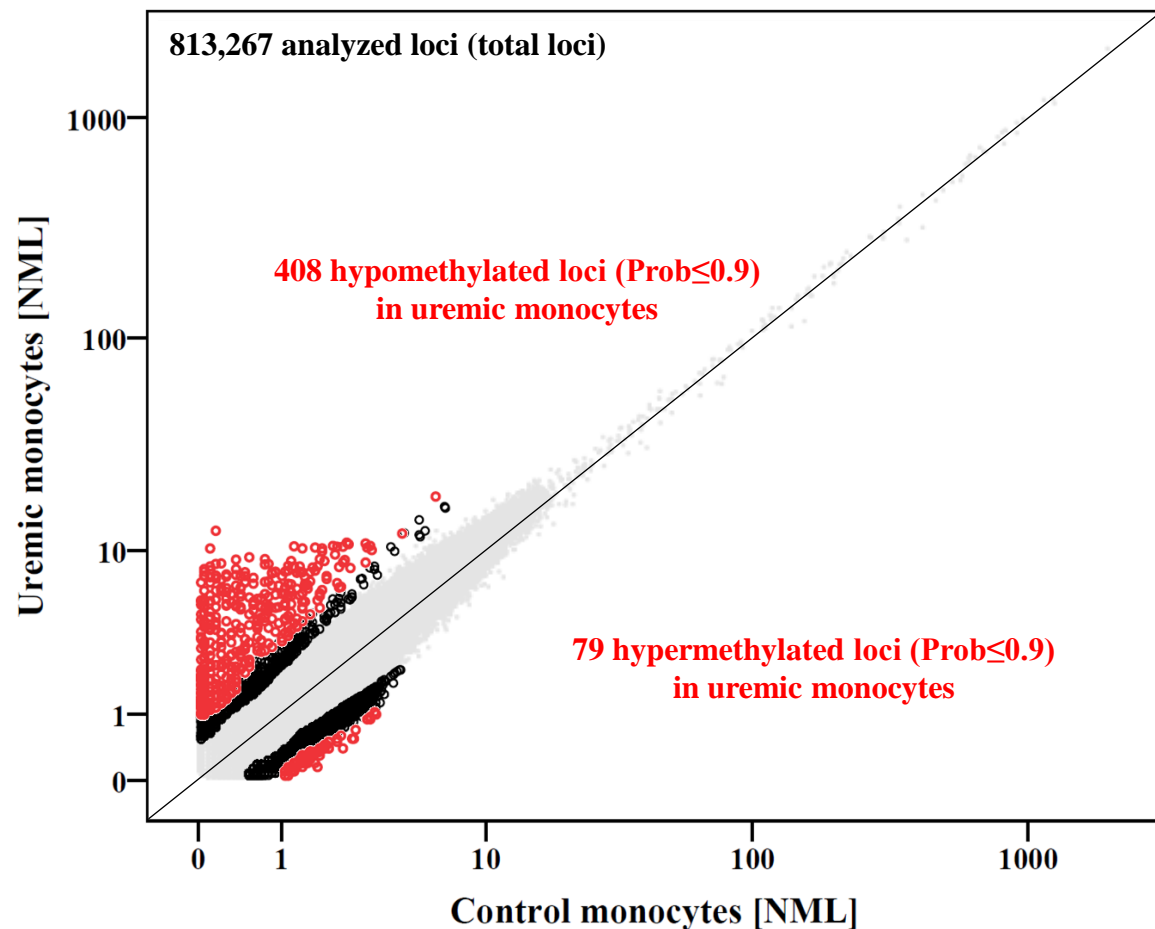


Figure S4

Total loci



Loci in CpG islands of gene upstream regions

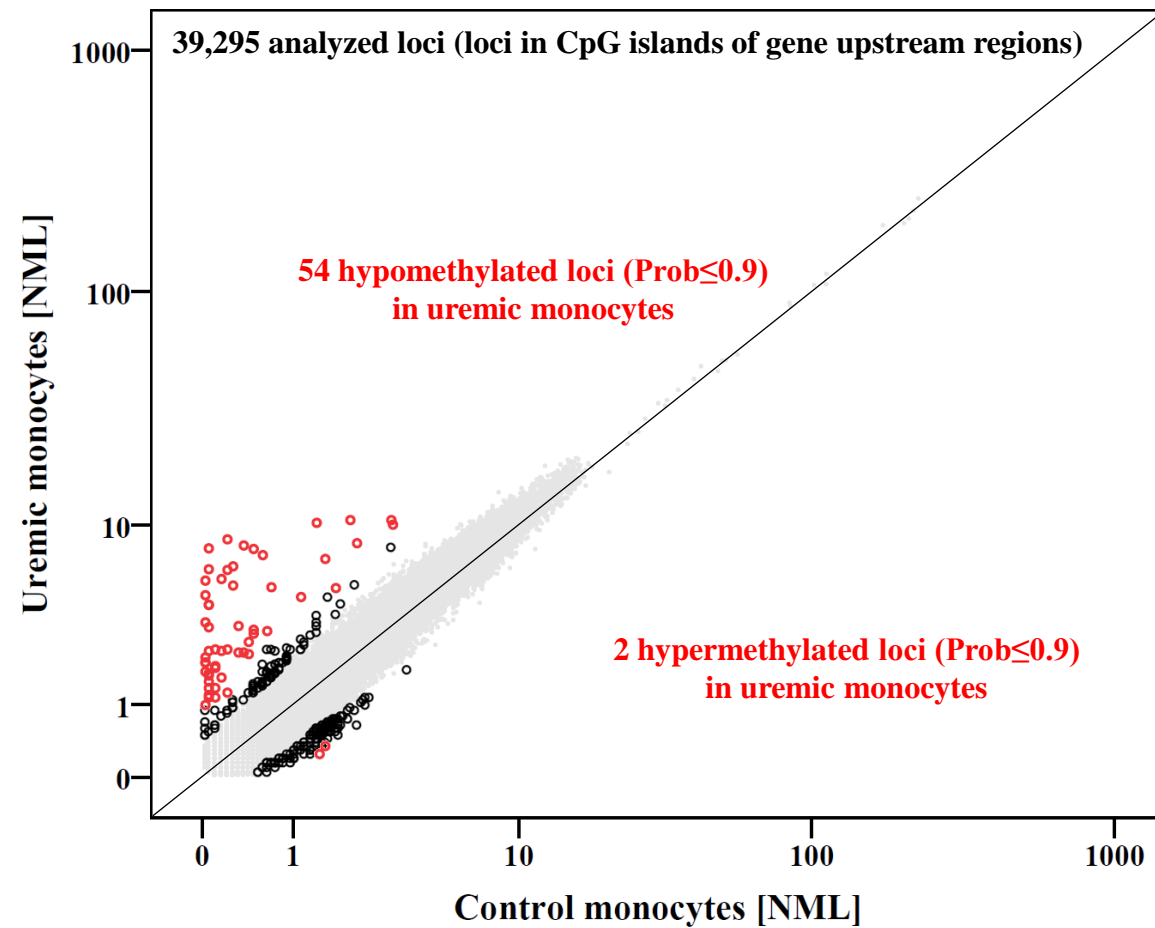
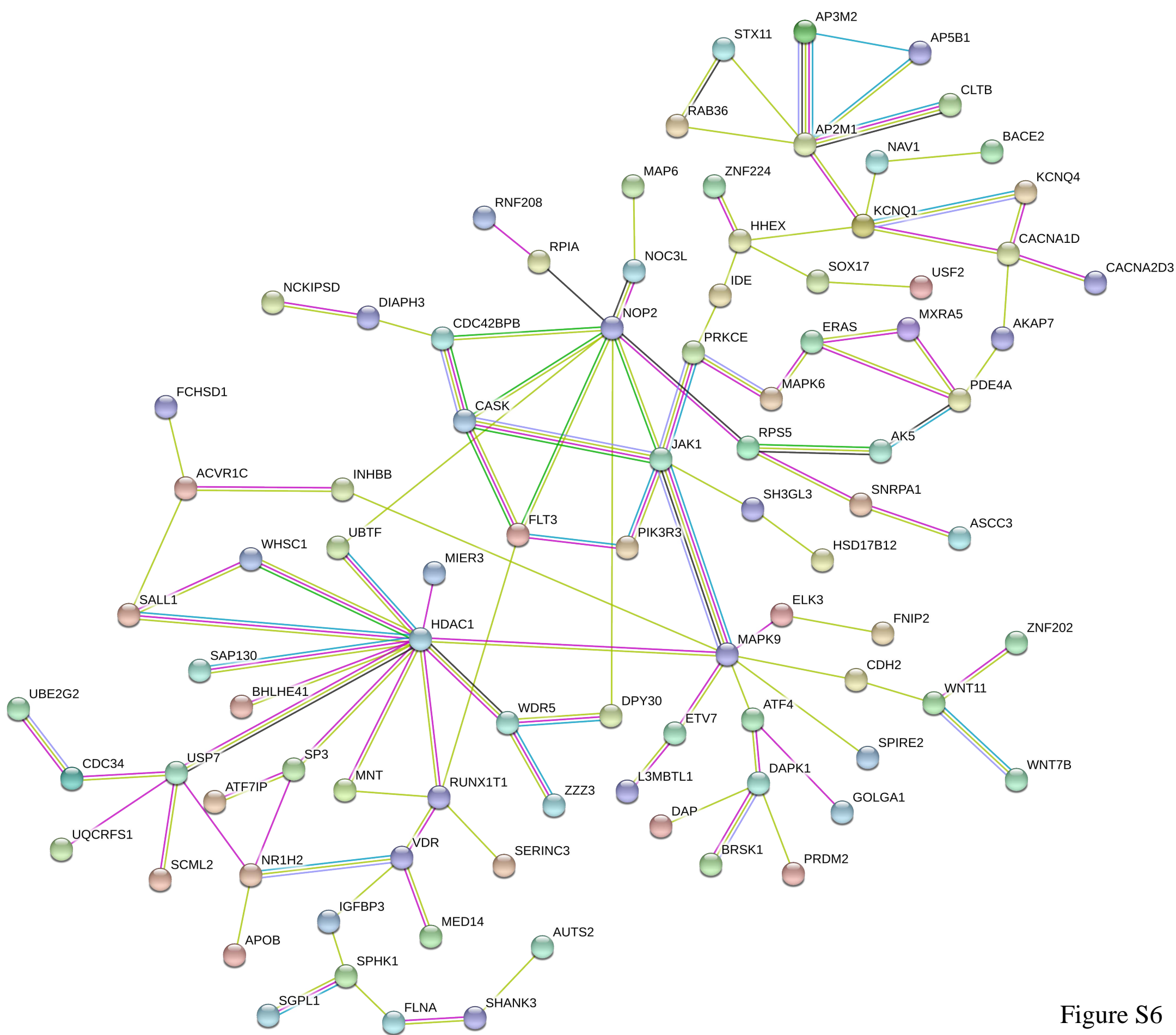


Figure S5



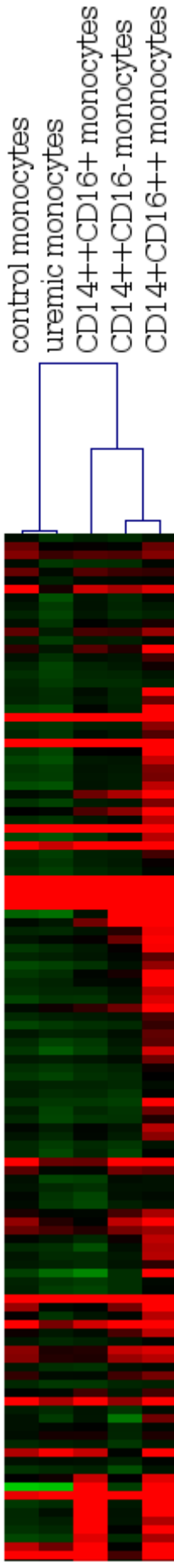


Figure S7

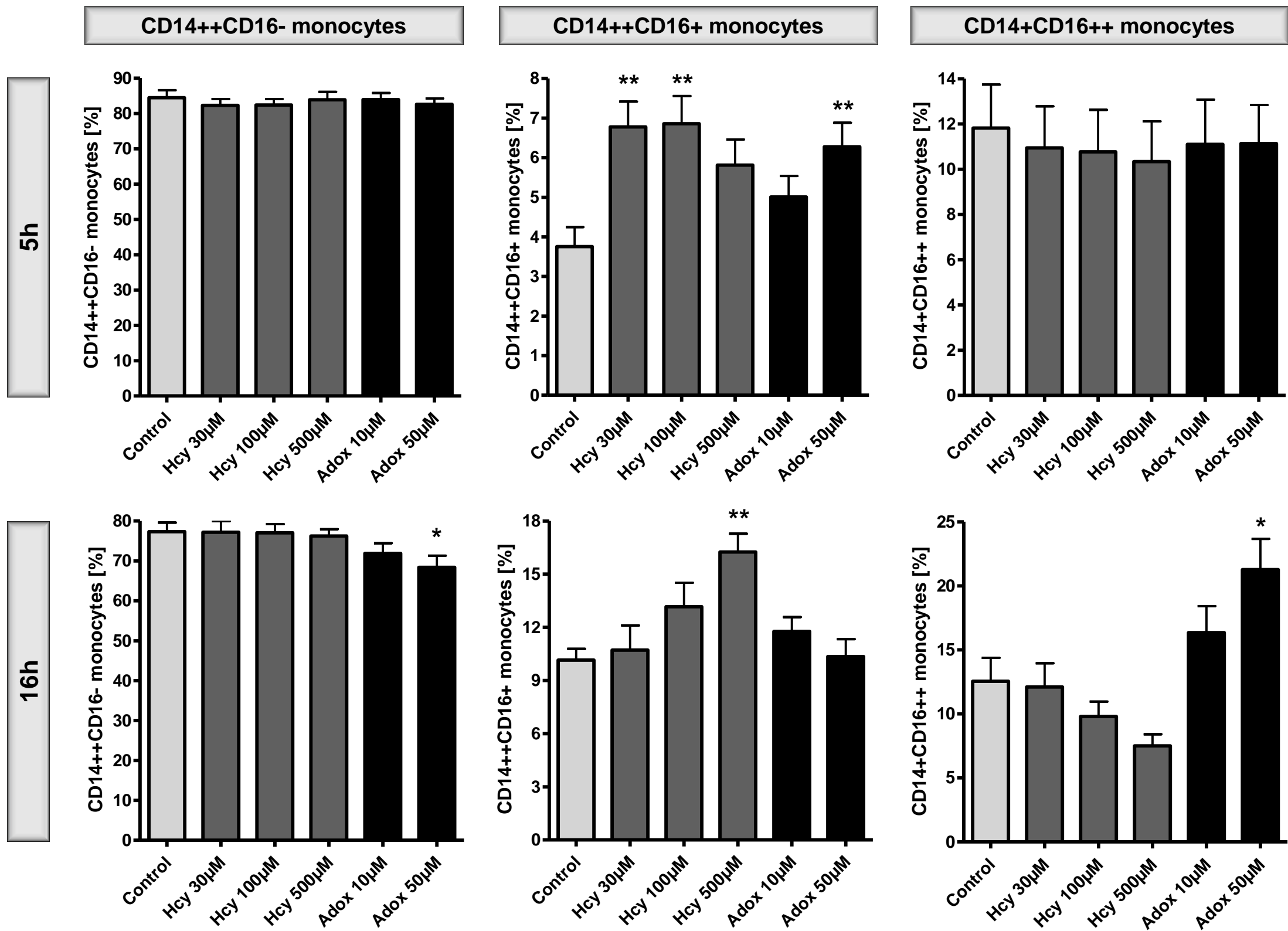


Figure S8

CD16 expression

CD86 expression

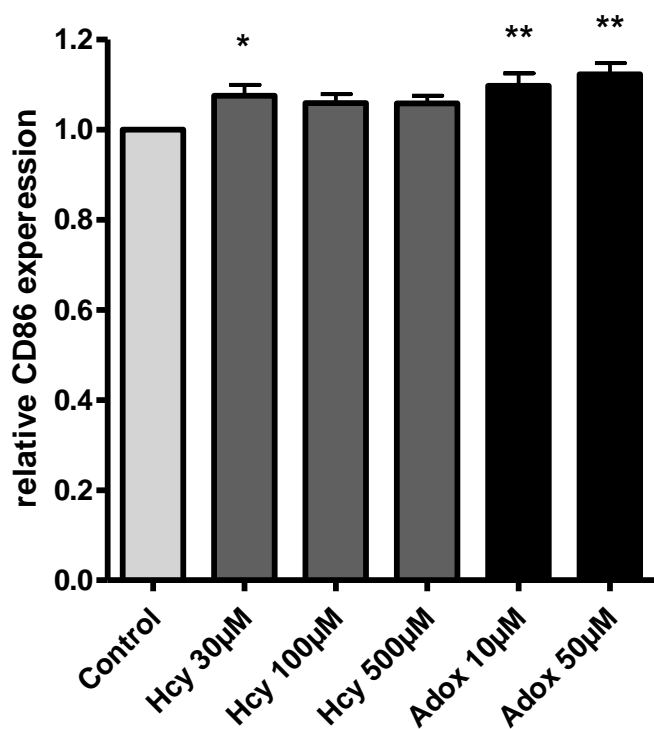
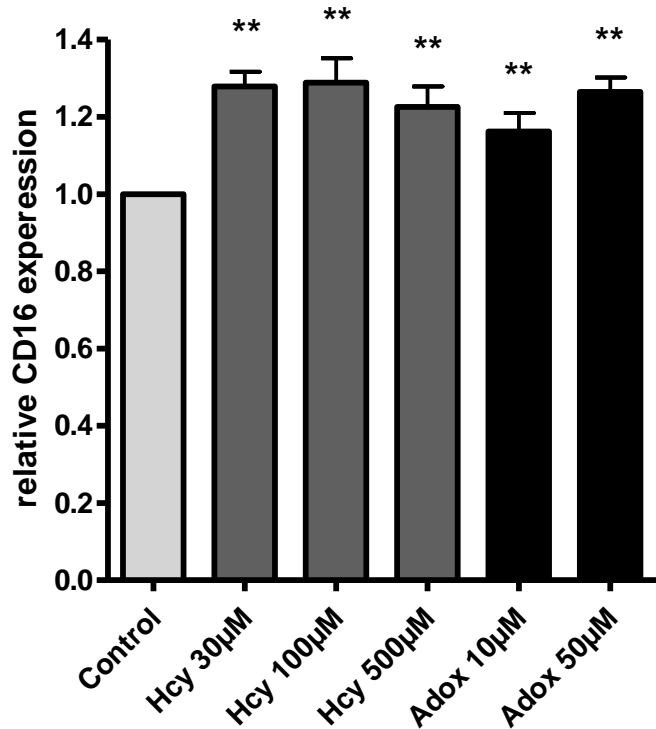


Figure S9

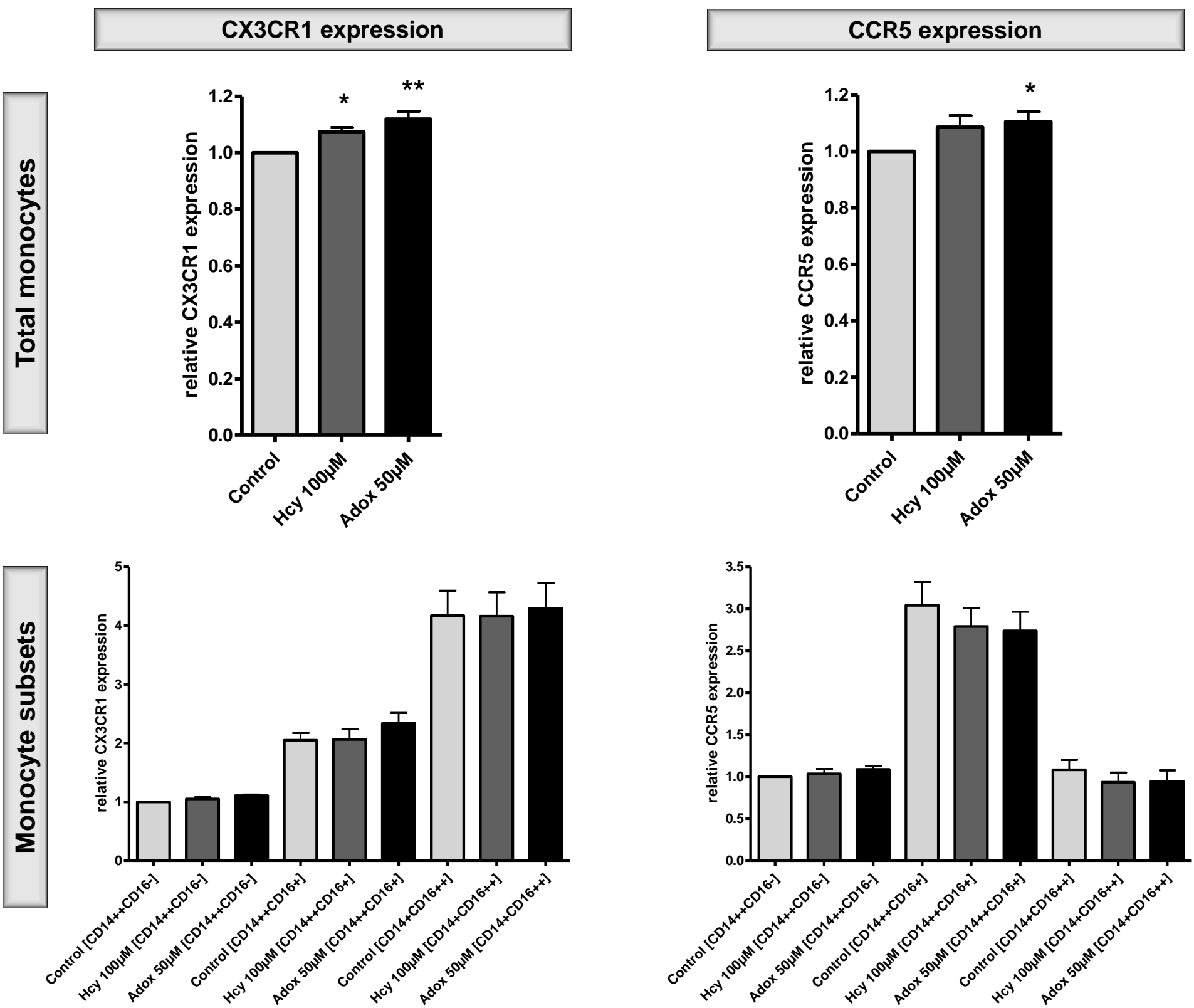


Figure S10

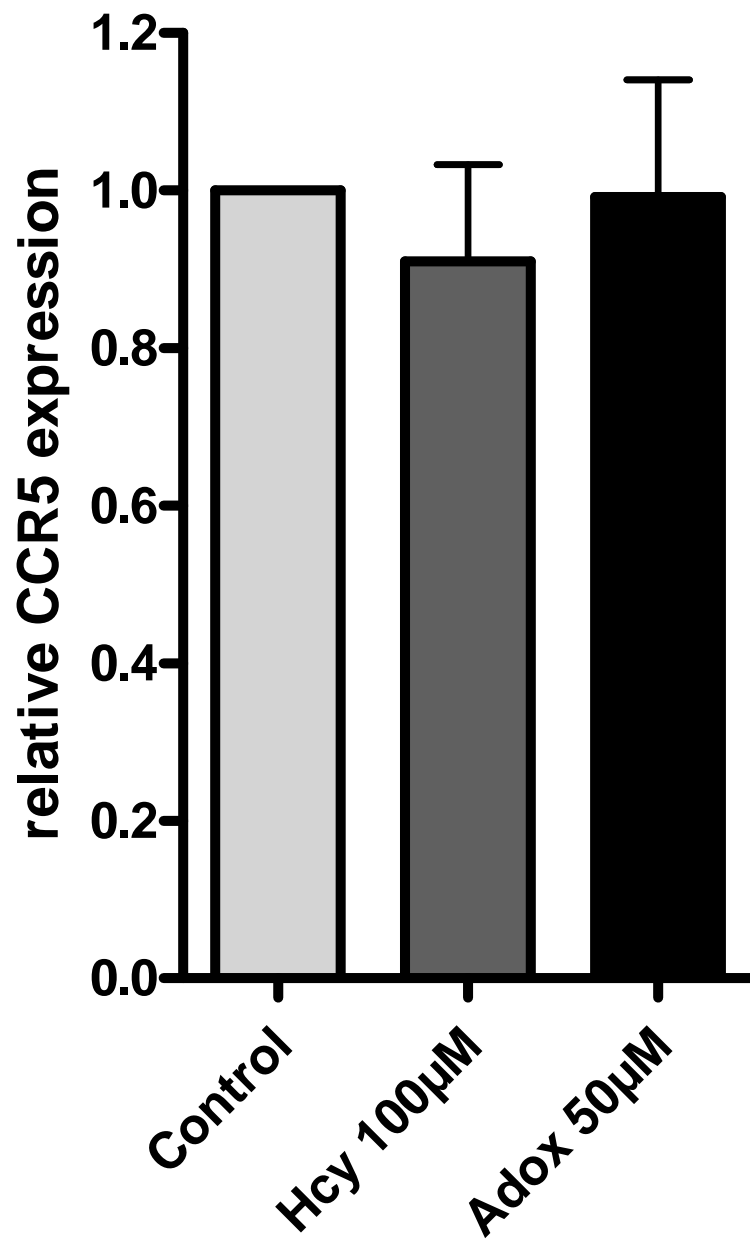
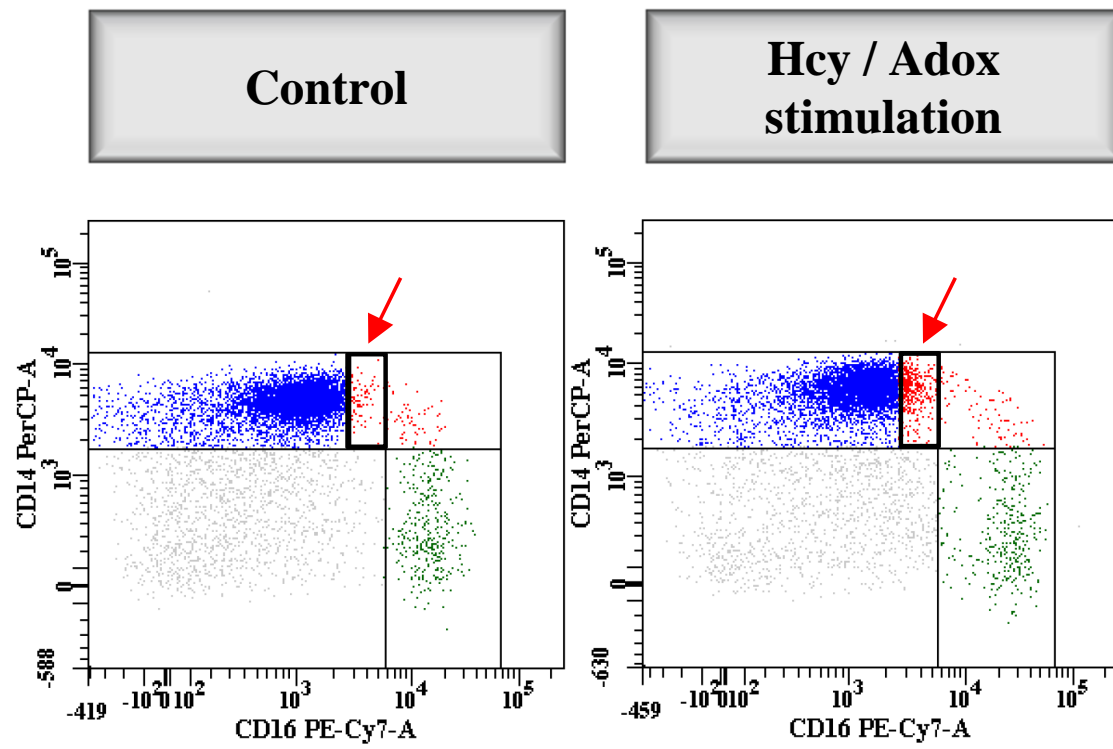
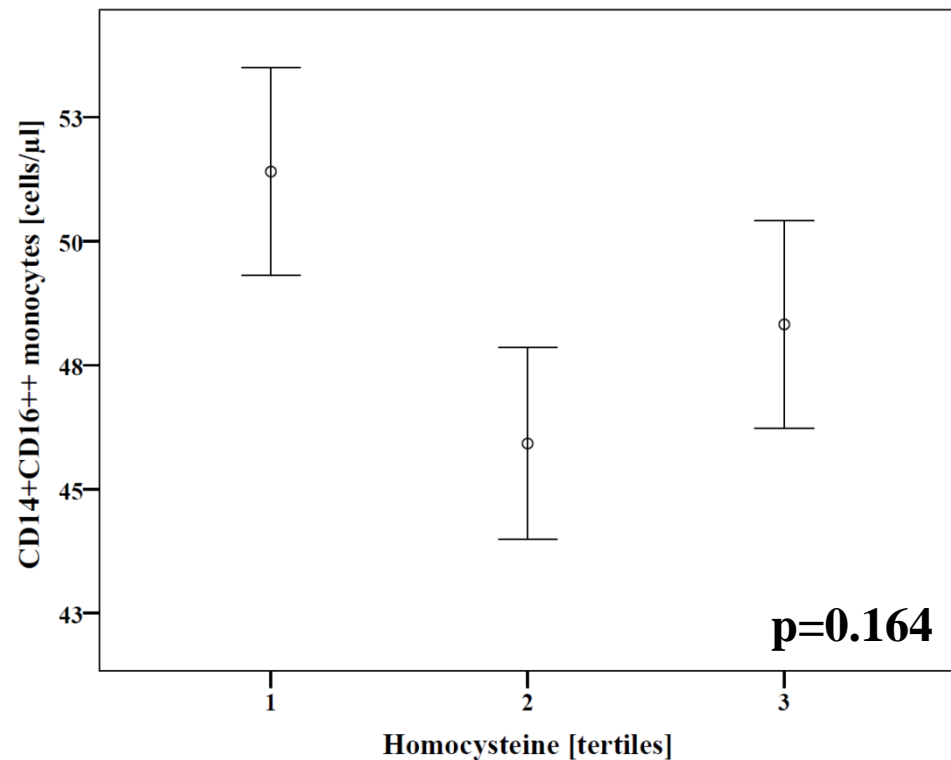


Figure S11

Homocysteine



S-Adenosylhomocysteine

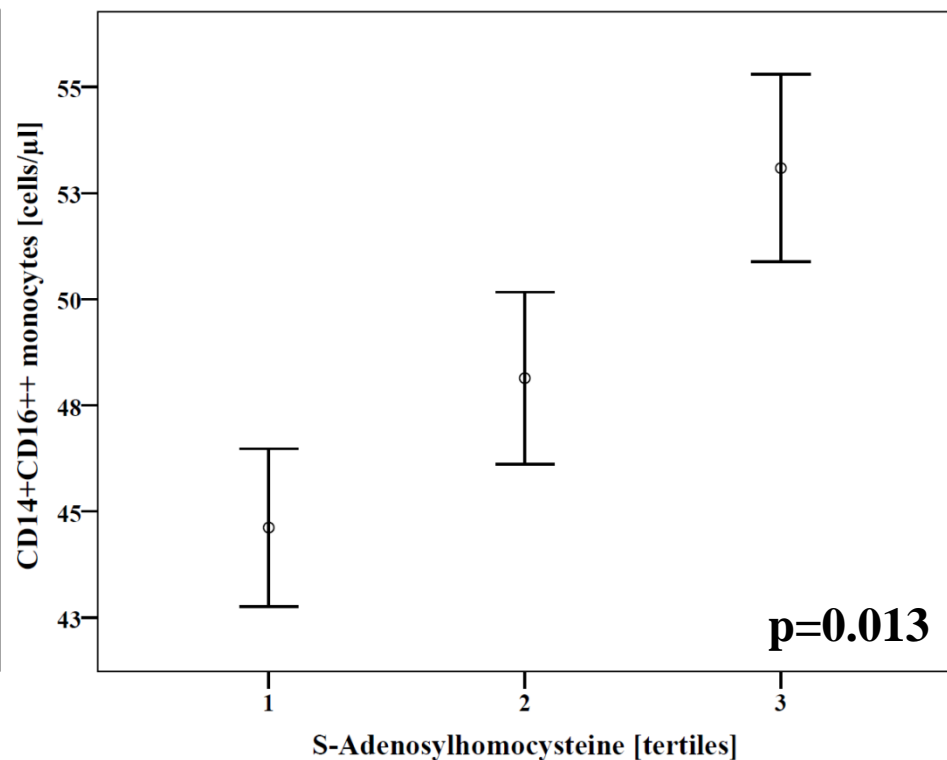


Figure S12

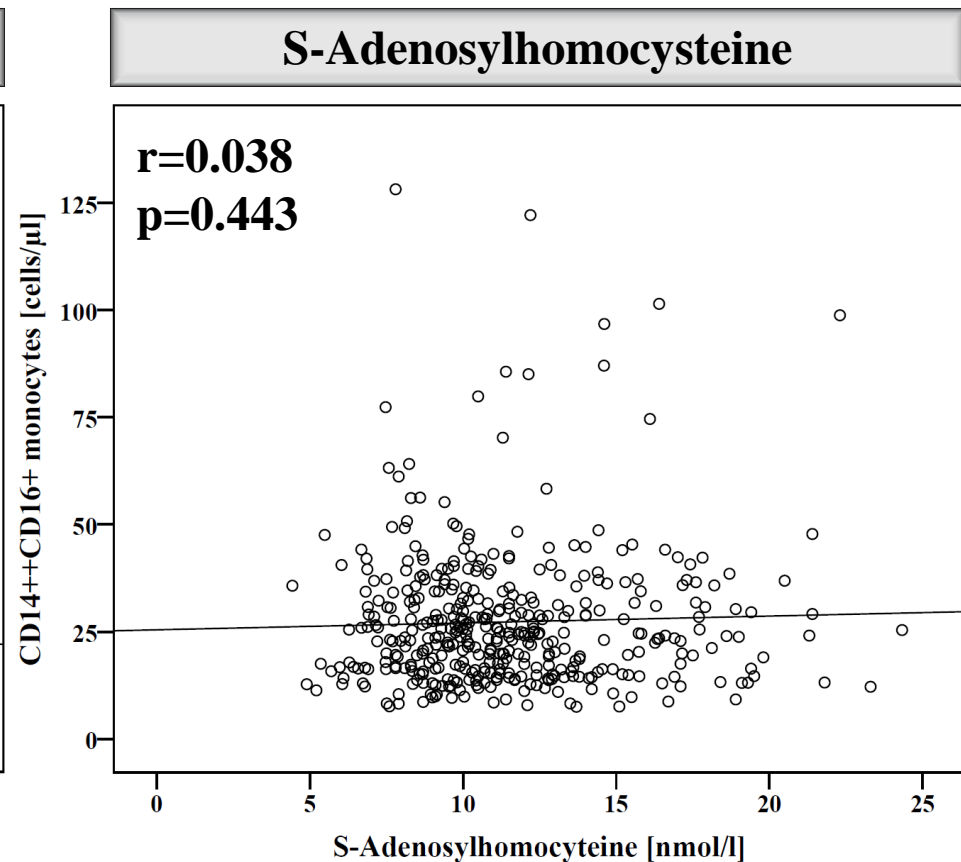
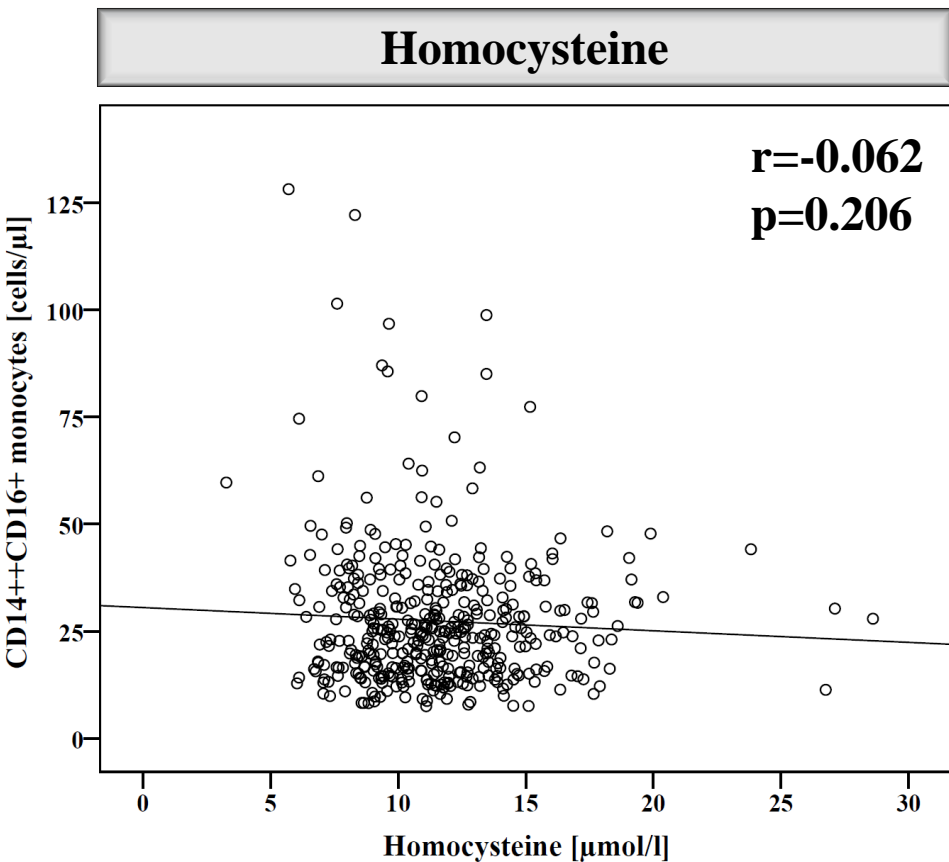


Figure S13